

## Preparation and upconversion properties of $\text{Er}^{3+}$ , $\text{Yb}^{3+}:\text{Y}_2\text{Si}_2\text{O}_7$ nanocrystallites embedded in PVA polymer nanocomposites

D. HRENIAK<sup>1\*</sup>, P. GŁUCHOWSKI<sup>1</sup>, W. STREK<sup>1</sup>, M. BETTINELLI<sup>2</sup>,  
A. KOZŁOWSKA<sup>3</sup>, M. KOZŁOWSKI<sup>3</sup>

<sup>1</sup>Institute of Low Temperature and Structure Research, Polish Academy of Sciences, 50-422 Wrocław, Poland

<sup>2</sup>Dipartimento Scientifico e Tecnologico, Università di Verona and INSTM, UdR Verona,  
Ca' Vignal, Strada Le Grazie 15, I-37134 Verona, Italy

<sup>3</sup>Wrocław University of Technology, Materials Recycling Center of Excellence, 50-422 Wrocław, Poland

The preparation of polymer nanocomposites consisting of a poly(vinyl) alcohol (PVA) network and  $\text{RE}^{3+}:\text{Y}_2\text{Si}_2\text{O}_7$  nanocrystalline particles ( $\text{RE} = \text{Yb}, \text{Er}$ ) is presented. Optical properties of the nanocomposites were preliminarily studied. In particular, efficient upconversion was observed in  $\text{Er}^{3+}$  and  $\text{Yb}^{3+}$  co-doped  $\text{Y}_2\text{Si}_2\text{O}_7$  nanoparticles embedded in the polymeric PVA host. It was found that the luminescence features of the  $\text{RE}^{3+}:\text{Y}_2\text{Si}_2\text{O}_7$  nanoparticles were affected by the polymeric host, resulting in a shortening of their luminescence lifetimes. This effect is discussed in terms of the effective refractive index.

Key words: *nanocomposite; luminescence; upconversion process; rare earths*

### 1. Introduction

A nanocomposite is a mixture of different component materials, in which at least one being of nanometer scale. Such materials may display combined features of all components or quite new properties resulting from mutual interactions between components. Organic-inorganic polymer composites have recently found wide technological applications. In the last years, a special interest has been focused on nanocomposites based on polymer networks involving nanoparticles being characterized by different electric, magnetic, or optical features. Different kinds of materials, among which are sulfides, organic compounds, and oxides nanocrystals, have been proposed

---

\*Corresponding author, e-mail: D.Hreniak@int.pan.wroc.pl

as nano-fillers in these composites [1, 2]. It is well known that yttrium disilicate doped with rare earth ions, especially  $\text{Eu}^{3+}$  and  $\text{Tb}^{3+}$ , is a very efficient phosphor material [3, 4]. Besides excellent luminescent properties, the morphology of these luminophors is important for perspective applications, and a spherical shape of the grains is preferred. For such applications, it is important to use particles not being aggregated and characterized by a narrow size distribution [5].

In the present paper, we report the preparation of polymer-based nanocomposites involving nanocrystalline  $\text{RE}^{3+}$ -doped  $\text{Y}_2\text{Si}_2\text{O}_7$  particles, where  $\text{Er}^{3+}$  and  $\text{Yb}^{3+}$  are chosen as the active ions. Our interest was primarily focused on the upconversion effect, resulting in visible emission after infrared excitation. Such an effect has found application in the development of upconversion lasers [6] and for the labeling of products [7, 8].

## 2. Experimental

In the first stage of the process, a nanopowder of  $\text{Y}_2\text{Si}_2\text{O}_7$  co-doped with 10% mol  $\text{Yb}^{3+}$  and 2%  $\text{Er}^{3+}$  ions was obtained. Tetraethoxysilane (TEOS), yttrium ( $\text{Y}_2\text{O}_3$ ), and rare-earth oxides ( $\text{Yb}_2\text{O}_3$  and  $\text{Er}_2\text{O}_3$ ) were used as the starting materials. Samples of the nanocrystalline powders were obtained using the preparation method of yttrium disilicate described elsewhere [9]. Yttrium and lanthanides nitrates were obtained by reacting stoichiometric amounts of their oxides with nitric acid. TEOS was hydrolyzed by stirring the mixture  $\text{Si}(\text{OC}_2\text{H}_5)_4\text{:H}_2\text{O:HCl}$  (in the volume ratio of 7.5:10:0.002) at 50 °C for 2 hours. The obtained sols were mixed with yttrium and lanthanides nitrates (dissolved in 10 ml of  $\text{H}_2\text{O}$ ) in a 1:1 molar ratio of ( $\text{Y} + \text{Yb} + \text{Er}$ ) to Si. The sols were left for one week at room temperature for gelation. After this time, the obtained wet gels were dried at 90 °C for a week. The cracked gels obtained during drying were annealed at 1100 °C for 4 h to yield the silicate in crystalline form.

The polymer used in the study was poly(vinyl alcohol) PVA (Kurray, Japan). Nanocomposites were prepared by a solution casting method. Initially, the polymer was dissolved in water with a concentration of 15 wt. %, after which the nanofiller was added. Finally, the suspension was mixed with a high shear rate. The resulting slurry was poured out on a flat surface with high surface tension and the solvent was removed by evaporation. The polymer nanocomposite and undoped matrix in the form of thin films with the thicknesses of 0.14  $\mu\text{m}$  and 0.10  $\mu\text{m}$ , respectively, were evaluated for their optical properties by means of luminescence investigations. The nominal volume fraction of nanoparticles embedded in the polymer was estimated to be ~2%.

Overall phase compositions were determined by X-ray powder diffraction with a Siemens D5000 diffractometer and  $\text{CuK}_{\alpha 1}$  radiation. The transmission spectrum was recorded using a Cary 5 spectrophotometer. Emission spectra were recorded, using a Jobin Yvon TRW 1000 spectrophotometer equipped with a laser diode (978 nm) as an excitation source, and a Hamamatsu R928 photomultiplier. Emission kinetics were measured with a Tektronics TDS 3052 oscilloscope, using an OPO laser system Continuum Surelite as the excitation source.

### 3. Results and discussion

Figure 1 shows the XRD pattern of the  $\text{Y}_2\text{Si}_2\text{O}_7$  nanopowder annealed at  $1100^\circ\text{C}$  in air. A well-defined  $\alpha\text{-Y}_2\text{Si}_2\text{O}_7$  structure was confirmed. Only a small shift in the diffraction peaks due to the replacement of  $\text{Y}^{3+}$  ions by smaller  $\text{Yb}^{3+}$  and  $\text{Er}^{3+}$  ions was observed. No structural impurities of other polymorphs of  $\text{Y}_2\text{Si}_2\text{O}_7$  were found. The size of the grains was determined using Scherrer's equation and gave the average of 40 nm. Analogous materials were also proven to be nanostructured by TEM measurements in our previous work [9].

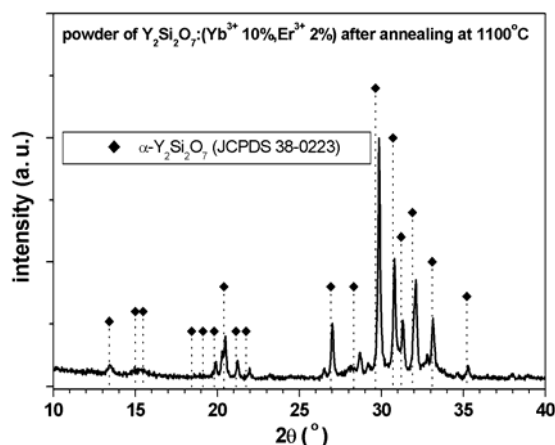


Fig. 1. XRD pattern of the  $\text{Y}_2\text{Si}_2\text{O}_7$  powder after annealing at  $1100^\circ\text{C}$

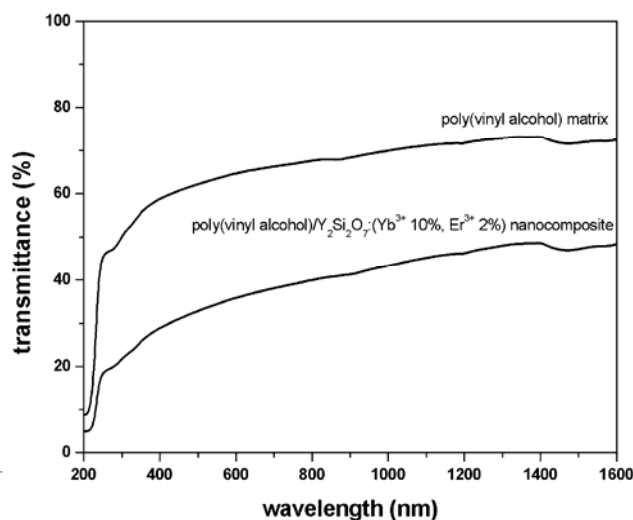


Fig. 2. Transmittance spectrum of a poly(vinyl alcohol) matrix and a poly(vinyl alcohol)/ $\text{Y}_2\text{Si}_2\text{O}_7:\text{Yb}^{3+} 10\%, \text{Er}^{3+} 2\%$  nanocomposite

The transmission spectrum of the PVA polymer film is shown in Figure 2. One can see that transparency in this kind of matrix in the examined spectral range is rela-

tively high and comparable to that reported elsewhere [10]. The ~10% lower transmittance observed here is due to surface roughness, resulting from the casting of the PVA film. A significant decrease in transmittance, observed for the composite sample, is due to Rayleigh scattering from the embedded particles (their average size was 40 nm). No attenuation due to the scattering effect could be expected for particles smaller than 15 nm [11]. Additionally, a part of the agglomerated grains, with sizes close to the used wavelength, can provide Mie scattering. There is still sufficient transmittance both for infrared excitation around 1  $\mu\text{m}$  and visible emission in the red spectral range. This means no important effects should appear in the emission characteristics due to light attenuation in the polymer matrix. In order to confirm this conclusion, the emission spectra of both the nanopowder and nanocomposite composed of the same nanopowder were recorded and compared.

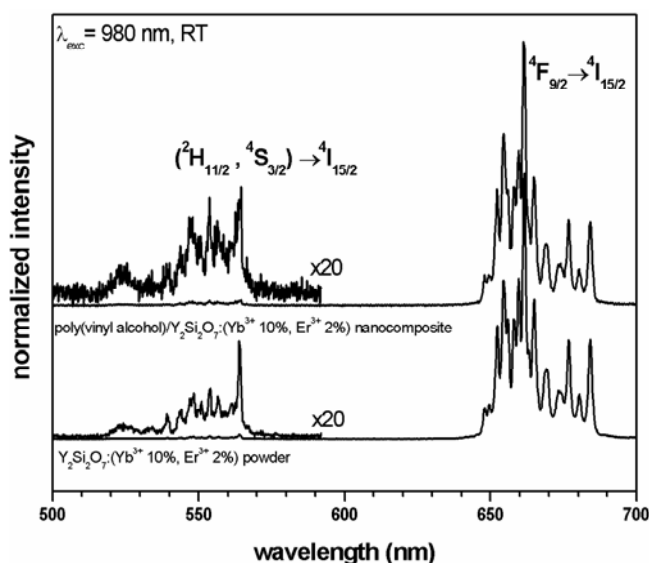


Fig. 3. Emission spectra of Er,Yb:Y<sub>2</sub>Si<sub>2</sub>O<sub>7</sub>:as-made powder (bottom) and embedded into PVA polymer (top)

The luminescence spectra of polymer nanocomposite films were measured at room temperature when excited with a IR laser diode operating at 980 nm (Fig. 3). It is well known that at this excitation energy (10 204  $\text{cm}^{-1}$ ) there is a very efficient upconversion from the excited level  $^2\text{F}_{5/2}$  of the Yb<sup>3+</sup> ion (~ 10200  $\text{cm}^{-1}$ ), populating the  $^2\text{H}_{11/2}$  level of the Er<sup>3+</sup> ion (~ 20400  $\text{cm}^{-1}$ ), converting IR excitation into visible light [12, 13]. According to this mechanism,  $^4\text{F}_{9/2}$  is populated by multiphonon relaxation from  $^4\text{S}_{3/2}$ . An additional upconversion mechanism directly populates the  $^4\text{F}_{9/2}$  level without populating either  $^2\text{H}_{11/2}$  or  $^4\text{S}_{3/2}$  [14]. The scheme of the upconversion mechanisms in the Er<sup>3+</sup> + Yb<sup>3+</sup> codoped material is shown in Fig. 4.

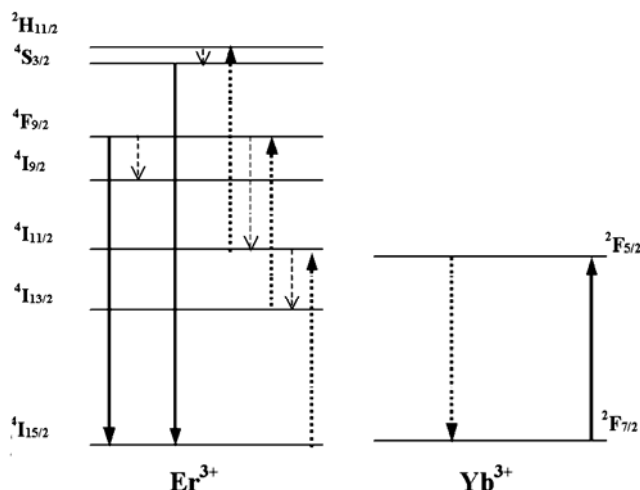


Fig. 4. Schemes of upconversion processes in the Er, Yb system

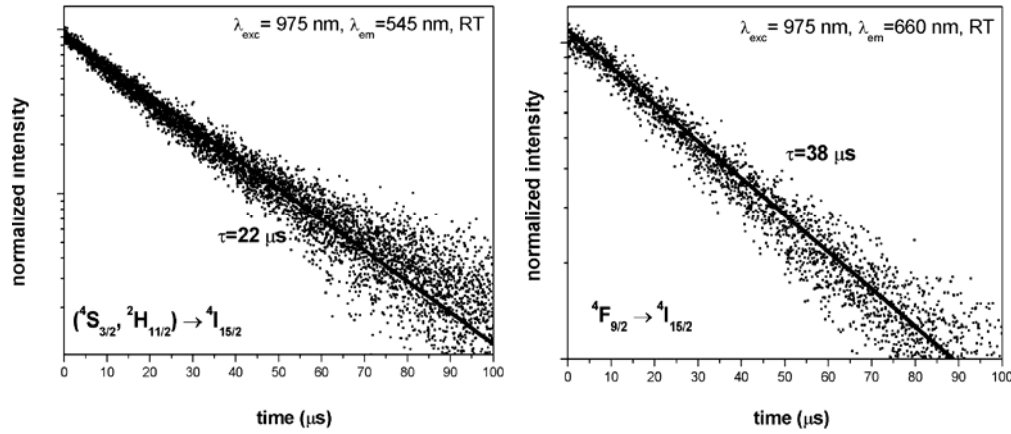
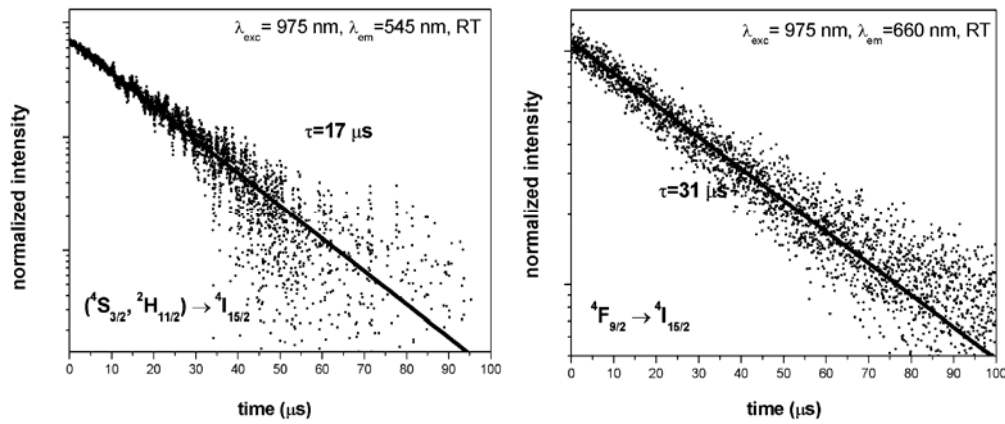
In the system under investigation, we have observed an efficient red luminescence centered at 670 nm, corresponding to the emission from the excited  $^4\text{F}_{9/2}$  to the ground level  $^4\text{I}_{15/2}$ . Moreover, a weak emission in the green range (540–560 nm), assigned to the  $(^2\text{H}_{11/2}, ^4\text{S}_{3/2}) \rightarrow ^4\text{I}_{15/2}$  transition, was recorded. The green emission is much weaker compared to the red one and was invisible with the naked eye. We measured the ratio of the integral red emission band intensity to the green band one,  $\beta$ , the ratio

$$\beta = \frac{I(^4\text{F}_{9/2} \rightarrow ^4\text{I}_{15/2})}{I(^4\text{S}_{3/2}, ^2\text{H}_{11/2} \rightarrow ^4\text{I}_{15/2})} \quad (1)$$

to be 32 for the nanocomposite, whereas for the nanopowder it was slightly higher (~43). This means that for the nanocomposite the intensity of the green emission decreased compared to the red one. We point out that the fine structure of the observed transition is identical for the nanopowder and nanocomposite, indicating that the sites accommodating the dopant ions are identical for the two materials.

To get insight into the role of the host in affecting the emission transitions of the  $\text{Er}^{3+}$  ion, we have measured the emission decay curves of the red and green transition bands of Er, Yb: $\text{Y}_2\text{Si}_2\text{O}_7$  nanopowders and polymer nanocomposite films. They were measured at room temperature under the excitation of an OPO laser operating at 975 nm (Figs. 5 and 6).

We found that the decay curves were almost perfectly exponential. The measured emission lifetimes, given in the figures, are significantly shorter for both transitions in the case of the polymer nanocomposite as compared to the nanopowder. The measured luminescence lifetime was reduced by 23% (from 22  $\mu\text{s}$  to 17  $\mu\text{s}$ ) for the more energetic  $(^2\text{H}_{11/2}, ^4\text{S}_{3/2}) \rightarrow ^4\text{I}_{15/2}$  transition, and by 19% (from 38  $\mu\text{s}$  to 31  $\mu\text{s}$ ) for the less energetic  $^4\text{F}_{9/2} \rightarrow ^4\text{I}_{15/2}$  transition.

Fig. 5. Luminescence decays of the Er,Yb:Y<sub>2</sub>Si<sub>2</sub>O<sub>7</sub> powderFig. 6. Luminescence decays of Er,Yb:Y<sub>2</sub>Si<sub>2</sub>O<sub>7</sub> embedded into PVA polymer

Since the Er<sup>3+</sup> ion is well-shielded from the high frequency vibration of the polymer, this behaviour indicates that the radiative decay rate of the dopant ions presumably increases for the polymer nanocomposite. Following recent results [15–18], we suppose that the host affects the radiative transition rate via enhancing the effective refractive index. The effective refractive index for nanocrystals embedded in host materials has been defined by Vetrone et al. [16] as

$$n_{\text{eff}}(x) = x n_{\text{Y}_2\text{Si}_2\text{O}_7} + (1-x) n_{\text{med}} \quad (2)$$

where  $x$  is the “filling factor” connected to the specific surface of the dispersed particles, illustrating the interface of nanocrystals and the medium, and  $n_{\text{med}}$  is the refractive index of the medium in which the nanocrystals are embedded. According to this relationship, given the refractive indices of the components ( $n_{\text{PVA}} \sim 1.5$  [19],  $n_{\text{Y}_2\text{Si}_2\text{O}_7} \sim 1.8$  [20],  $n_{\text{air}} = 1$ ), the effective refractive index for nanocrystals of Y<sub>2</sub>Si<sub>2</sub>O<sub>7</sub> dis-

persed in PVA should be higher than for nanopowders in air (assuming a high surface of the powder, as observed in [16]). It can be easily checked that for each  $x \neq 0$  used,  $n_{\text{eff}}$  (for  $n_{\text{med}} > 1$ ) is higher than  $n_{\text{eff}}$  in air. As a result, by using  $n_{\text{eff}}$  in the place of  $n$  [21], the radiative lifetime  $\tau_R$  of the electric dipole transitions, can be expressed as

$$\tau_R \propto \frac{1}{f(\text{ED})} \frac{\lambda_0^2}{\left[ \frac{1}{3}(n^2 + 2) \right]^2 n} \quad (3)$$

$$\tau_R \propto \frac{1}{f(\text{ED})} \frac{\lambda_0^2}{L} \quad (4)$$

where

$$L = \left[ \frac{1}{3} \left( \left( n_{Y_2Si_2O_7} + (1-x)n_{\text{med}} \right)^2 + 2 \right) \right]^2 \left( n_{Y_2Si_2O_7} + (1-x)n_{\text{med}} \right) \quad (5)$$

and where  $f(\text{ED})$  is the oscillator strength for the electric dipole transition,  $\lambda_0$  is the wavelength in vacuum, and  $n$  is the refractive index of the material.

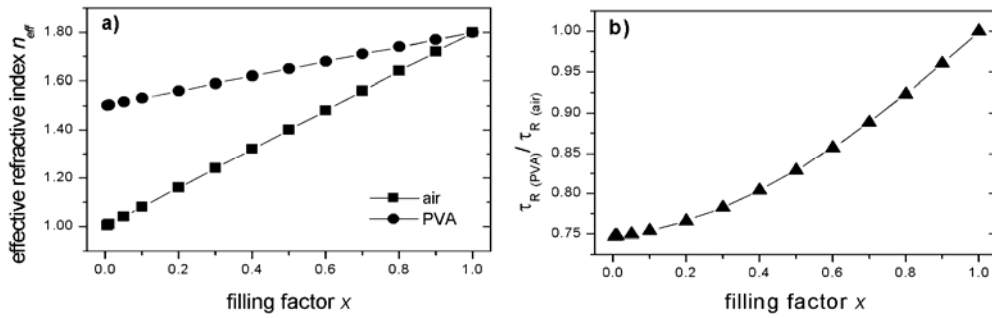


Fig. 7. Dependence of the calculated effective refractive index  $n_{\text{eff}}$  (a) and change in radiative lifetimes  $\tau_{R(\text{PVA})}/\tau_{R(\text{air})}$  (b) on the filling factor  $x$

The radiative lifetime should be lower for the composite material than for the nanocrystalline powder in air. Assuming that only  $L$  is a variable in Eq. (4) and that the surface areas of the powder nanocrystals PVA are the same, we can find how the radiative lifetime changes by changing  $n_{\text{med}}$  from 1 ( $n_{\text{air}}$ ) to 1.5 ( $n_{\text{PVA}}$ ). The calculated dependence of the effective refractive index  $n_{\text{eff}}$  and calculated relative change of radiative lifetimes  $\tau_{R(\text{PVA})}/\tau_{R(\text{air})}$  on a filling factor  $x$  is plotted in Figure 7. It was estimated that the observed change in the luminescence lifetime of  $\sim 20\%$  could correspond to  $x \approx 0.4$ .

## 4. Conclusions

The purpose of the present work was to obtain transparent polymer films with embedded nanocrystallite powder anti-Stokes luminophores, demonstrating efficient up-conversion luminescence under infrared excitation. Such nanocomposite films can be used for optoelectronic devices and security systems. As the nanocrystalline luminophores, yttria disilicate ( $\text{Y}_2\text{Si}_2\text{O}_7$ ) doped with Yb and Er ions were chosen. The fabrication of Er,Yb: $\text{Y}_2\text{Si}_2\text{O}_7$ :PVA polymer nanocomposite materials was described. Their morphology and optical transparency were determined. In particular, the up-conversion luminescence of  $\text{Er}^{3+}$  after exciting  $\text{Yb}^{3+}$  with an infrared laser diode was investigated. The up-conversion spectra of Er,Yb: $\text{Y}_2\text{Si}_2\text{O}_7$ :PVA, manifested by two  $\text{Er}^{3+}$  luminescence transition bands in the red and green range, were similar to those measured for the nanocrystalline powder, in spite of the fact that the luminescence decay times were significantly decreased. The process was discussed in terms of the host effect enhancing the effective refractive index. A method for estimating the filling factor from relative changes in luminescence lifetimes for nanopowders in air and embedded in host materials was proposed.

## Acknowledgements

This work was supported by KBN grant PBZ-KBN-095/T08/2003. We would like to thank Dr. M. Wołczyr for the XRD measurements and Dr. P. Solarz for his help in the luminescence decay measurements.

## References

- [1] RAY S.S., OKAMOTO M., Prog. Polym. Sci., 28 (2003), 1539.
- [2] KICKELBICK G., Prog. Polym. Sci., 28 (2003), 83.
- [3] CHOI Y.Y., SOHN K.-S., PARK H.D., CHOI S.Y., J. Mater. Res. 16 (2001), 881.
- [4] ZHANG Q.Y., PITA K., BUDDHUDDU S., KAM C.H., J. Phys. D. App. Phys., 35 (2002), 3085.
- [5] KANG Y.C., LENGGORO I.W., PARK S.B., OKUYAMA K., J. Solid State Chem., 146 (1999), 168.
- [6] SCHEIFE H., HUBER G., HEUMANN E., BAR S., OSIAC E., Opt. Mater., 26 (2004), 365.
- [7] SUYVER J.F., AEBISCHER A., BINER D., GERNER P., GRIMM J., HEER S., KRAMER K.W., REINHARD C., GÜDEL H.U., Opt. Mater., 27 (2005), 1111.
- [8] PODBIELSKA H., STRĘK W., Proc. SPIE 3314 (1998), 247.
- [9] HRENIAK D., STRĘK W., OPALIŃSKA A., NYK M., WOŁCZYRZ M., ŁOJKOWSKI W., MISIEWICZ J., J. Sol-Gel Sci. Techn., 32 (2004), 1.
- [10] ABD EL-KADER K.A.M., ABDEL HAMIED S.F., J. Appl. Polym. Sci., 86 (2002), 1219.
- [11] BRAUN M.M., PILON L., Thin Solid Films 496 (2006), 505.
- [12] SCHEPS R., Prog. Quant. Electr., 20 (1996), 271.
- [13] CHENG Z.X., ZHANG S.J., SONG F., GUO H.C., HAN J.R., CHEN H.C., J. Phys. Chem. Solids 63 (2002), 2011.
- [14] CHEN X., NGUYEN T., LUU Q., DI BARTOLO B., J. Lumin. 85 (2000), 295.
- [15] YANG H.S., HONG K.S., FEOFILOV S.P., TISSUE B.M., MELZER R.S., DENNIS W.M., J. Lumin., 83–84 (1999), 139.
- [16] MELTZER R.S., HONG K.S., Phys. Rev. B, 61 (2000), 3396.
- [17] SCHNIEPP H., SANDOGHDAR V., Phys. Rev. Lett., 89 (2002), 257403.



- [18] VETRONE F., BOYER J.-C., COPOBIANCO J.A., SPEGHINI A., BETTINELLI M., *Nanotechnology*, 15 (2004), 75–81.
- [19] KUMAR R., SINGH A.P., KAPOOR A., TRIPATHI K.N., *Opt. Eng.*, 43 (2004), 2134.
- [20] CHING W.Y., OUYANG L., XU Y.-N., *Phys. Rev. B*, 67 (2003), 245108.
- [21] MELTZER R.S., FEOFILOV S.P., TISSUE B.M., YUAN H.B., *Phys. Rev. B*, 60 (1999), R14012.

*Received 30 September 2005*

*Revised 21 February 2006*